Advances in Science and Technology Research Journal

*Advances in Science and Technology Research Journal*, 2025, 19(7), 338–345
https://doi.org/10.12913/22998624/204278
ISSN 2299-8624, License CC-BY 4.0

Received: 2025.03.21
Accepted: 2025.05.15
Published: 2025.05.25

# Assessment of induced residual stresses and microstructure of Al/B4C/FA composite extruded by equal channel angular pressing

Tiba Qahtan Irhayyim[1*], Jabbar Gattmah[1]

[1] Department of Material Engineering, College of Engineering, University of Diyala, 32001, Baqubah, Diyala, Iraq
* Corresponding author's e-mail: teebaqahtan99@gmail.com

## ABSTRACT

This research evaluates the residual stresses and microstructure of rods fabricated from a hybrid aluminum matrix composite (Al1050/$B_4C$/FA). The rod composite is subjected to various passes (cycles) using equal channel angular pressing (ECAP) at room temperature. Channel angles of 120° and 135° with pass numbers of 1P, 2P, 3P, 4P, 5P, and 6P are used to investigate the induced residual stresses (IRS) and examine the microstructure. The destructive cutting technique (CT) is employed to assess the state of IRS in the axial direction, and scanning electron microscopy (SEM) is used to check the microstructure before and after severe plastic deformation (SPD). The results show that the values of residual stresses tend to increase due to the effects of SPD compared to the casting composite. As the ECAP cycles increase, the magnitudes of residual stresses start to change; the compressive state of residual stresses is near the rod surface, while the stresses are in tensile state near the center of the composite rod. The cycles of ECAP significantly impact the grain size reduction. The smallest grain size is observed at a die angle of 120° after 6 ECAP passes, measuring between 1 and 8 µm, while the grain size for the casted rods ranged from 4 to 15 µm.

**Keywords:** Al1050/$B_4C$ /FA composite, equal channel angular pressing, cutting technique, residual stresses, microstructure.

## INTRODUCTION

Hybrid aluminum is a material composite that combines aluminum alloy as a matrix with other materials such as steel, polymers, ceramics, etc. Hybrid aluminum has drawn much attention from various engineers due to its excellent physical and mechanical properties, like high strength compared to weight and low cost, which led to its wide use in different industrial applications (1). Also, many task features of the hybrid composites of the aluminum metal matrix, such as ductility, malleability, and corrosion resistance improvements, make it unique in naval and military air uses. The material forming operation using equal channel angular pressing (ECAP) proved to be a reliable production process in enhancing microstructure by refining the grains of the metal composite and improving mechanical properties (2). All metal forming processes conducted under room conditions, like drawing, extrusion, rolling, and ECAP, produce high plastic deformations that generate residual stresses. These stresses are considered defects created inside the material and effectively influence the fatigue life (3–6). Therefore, there is an important need to increase the research based on experimental methods to manufacture high-quality hybrid aluminum composites. El Aal et al. (7) processed pure Al 1080 samples up to ten passes at room temperature by ECAP to improve corrosion, mechanical, and microstructural properties. Lokesh et al. (8) evaluated the impact of ECAP on grain refinement and mechanical characteristics of hybrid composite, including aluminum with graphite and silicon carbide (Al6061/Gr/SiC) produced by stir casting operation. Lee et al. (9) determined the residual stress behavior in Cu billet formed by ECAP after 1 pass using neutron diffraction and FEM. The results show a nonuniform state of residual stresses from the lower to the upper zone of a billet. Although nonuniformity of residual stresses, the middle region of the billet had relatively homogeneous tensile RS. Bharath et al. (10) studied the effect of SPD on Al 2618/SiC/E-glass fibers prepared by the stir casting method, then ECAP was conducted at environment temperature based on 1 cycle with a channel angle of 90°. Romero-Resendiz et al. (11) characterized the mechanical, microstructural, and residual stress states of aluminum grade 2017 extruded by ECAP at 200 °C. The highest microhardness and grain refinement were found after the first pass, while the residual stresses (RS) gave tensile behavior at 1 pass and compression value from 3 to 6 passes. Sureshkumar et al. (12) extruded hybrid aluminum samples reinforced by Cu(NO2)3)p and (β-Si3N4) p to evaluate mechanical properties and microstructure features. Hou et al. (13) checked the microstructure of pure Al processed by ECAP 90° die with various cycles. The results illustrate that grain refinement occurs after the ECAP operation, and the grains are most uniform at pass 8, with a maximum value of tensile strength and hardness in the first pass of ECAP. Güler et al. (14) synthesized graphene Nanosheets by the liquid phase exfoliation process and added them into the aluminum matrix, then ECAP was applied at two die angles of 120° and 90° to enhance microstructure and mechanical features. The tensile strength rises with augmenting ECAP passes, while ductility significantly decreases. Shivashankara et al. (15) investigated the influence of ECAP using a die angle of 90° up to four cycles (passes) with route BC on the mechanical characteristics of Al 7068 alloy at 200 °C to enhance the hardness and ultimate tensile strength by ECAP. Al-Alimiet al. 2021 (16) applied different ECAP passes to asses physical and mechanical properties of a composite made of mixing recycled Al6061 aluminum chips with boron carbide reinforcements. Agarwa et al. (17) studied and examined the mechanical behavior of pure Al compressed by the ECAP tool with the best factor of die design. The grain refinement from 530 to 220 nm was reduced, and tensile strength was reached 386 MPa after three cycles of ECAP. Sureshkumar et al. (18) checked the electrochemical corrosion of AA6063/ $Si_3N_4$/$Cu(NO_3)_2$ manufactured employing the stir casting method and extruded by ECAP. The rate was decreased by 63% after ECAP, while wear resistance was found to be 73% higher than as cast composite, and a 40.7% reduction in the friction coefficient. Sathi et al. (19) used aluminum matrix composites reinforced with three types of red mud using stir casting and then subjected to ECAP for evaluation of wear and structural behavior. The loss of wear was decreased after ECAP due to the reduction in grain size. Tolcha et al. (20) evaluated the tensile strength, hardness, and grain size of 6061 manufactured by the casting process and processed by ECAP. Hassan et al. (21) subjected rods of hybrid aluminum composite Al1050/ $Al_2O_3$/Gr to severe plastic deformation using ECAP with different passes and channel die angles of 120° and 135° to improve microstructure and mechanical properties. They revealed that the cycle number of ECAP strongly affects grain refinements, hardness, and tensile strength.

Many researchers have studied residual stresses and the microstructure of hybrid metal matrix composites, while a rare few works have investigated the effect of ECAP on residual stress and microstructure of Al1050/ $B_4C$/FA, which refers to aluminum, boron carbide, and fly ash. Although using ECAP improves mechanical features and microstructure characteristics, the residual stresses IRS within the material are generated due to severe plastic deformation SPD. In this study, Al1050/$B_4C$/FA composite manufactured by stir casting operation is adopted to be subject to SPD with ECAP passes of 1, 2, 3,4,5, and 6 at die angles of 120° and 135°. The IRS in the axial direction is measured using the destructive procedure based on the CT, as well as the microstructure characteristics are examined utilizing SEM.

## MATERIALS AND METHODS

In this work, the initial materials are the hybrid aluminum matrix composite rods (Al1050/ $B_4C$/FA), fabricated by the stir casting method, consisting of 93% 1050 pure aluminum as matrix, 2% boron carbide, and 5% fly ash incorporated as reinforcement materials. The casting temperature between 650° and 750° was applied with a mixing time of 2 min at a speed of 650–810 rpm. The argon gas was used to prevent oxidation during the process. The dimensions of the casted rods are represented in a length of 12 cm and a diameter of 1.2 cm. The combination of these materials affords superior mechanical properties with lightweight for pure aluminum and boron carbide ($B_4C$) hard material with a high melting point. Boron carbide is an eligible material for strengthening because of its high hardness, as well as having better mechanical properties with low density. Energy consumption, toxic gas emissions, and cost were reduced by incorporating fly ash into aluminum composites (22). Fly ash (FA) is a cheap and low-density material that improves the durability and strength of hybrid aluminum metal composites (HAMCs) (23). The elements of the pure aluminum grade 1050 in terms of chemical composition are introduced in Table 1 (21). The decrease in defects and an increase in the specific area of the composite can be obtained with small particles. The grain size of $B_4C$ particles with a purity of 99% is 40–46 µm, while the fly ash particle size is 44 µm.

Figure 1 shows the elements of the initial composite obtained by energy-dispersive spectrometry examination (EDS test). It can be noticed that the base material is Al with other elements including O, C, Fe, Ca, and Ti. On the other hand, the boron element can not be seen due to its low atomic weight, which makes it difficult to expose during examination (24).

The ECAP die is made of tool steel and includes two circular channels with a diameter of 1.2 cm and different channel angles of 120° and 135°. The twelfth samples were prepared to be subject to SPD, 6 of them were pressed in ECAP at a die angle of 120°, and the other were processed at a channel angle of 135°. Firstly, the Al1050/$B_4C$/FA rods were cut to a diameter of 1.2 cm and a length of 9 cm. Then, the die channels and samples were lubricated using grease (lubricating grease) to minimize the friction between the sample surface and the channel wall of ECAP. The ECAP parts were fixed using the torque wrench to ensure the tightening of the bolts, which gives more accurate and successful deformation results, and the billet can flow easily through the die channels. Finally, the assembly parts were placed under the pressing device (Universal tensile testing machine), which has a maximum capacity of 1000 kN. In this test, the load rate of 0.25 kN/s was applied at room temperature for all experiments. After passing through the channels of the ECAP die, the two dies were dismantled to separate the rod from the ECAP.

This study adopted a destructive procedure employing the CT to determine the strain inside the rod composite based on strain gages. The principal residual stress measurements using CT depend on the cutting of the rod in a circumferential direction, and then the strain was recorded based on the axial direction. The installation of strain gages on the surface of the rods and determining their directions were considered the most important tasks that can give accurate results. All grease, dust, and rust were carefully removed from the surface of the rod composite, then acetone was used to clean the zone glue. After that, an adhesive type (total tools super glue adhesive THT3521) was utilized to stick the strain gages on the surface in the middle of the sample (4.5 mm from the rod edge). Then, the strain gage was covered with epoxy resin glue resistant to high temperature and vibration. At the same time, it prevents thermal stress and isolates the strain gage from any chips or coolant liquid induced through the cutting operation. The strain gage type (GB/T13992-2010) with 3 mm length,

**Table 1.** The elements of pure Al grade 1050

| Al1050 | Si | Fe | Cu | Mn | Mg | Cr | Zn | Al |
|---|---|---|---|---|---|---|---|---|
| Element % | 0.064 | 0.155 | 0.004 | 0.004 | 0.004 | 0.004 | 0.008 | Bal. |

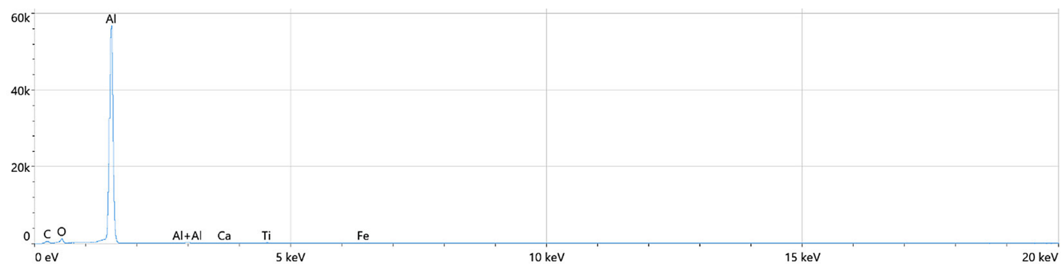


**Figure 1.** Element ratio of Al1050/$B_4C$/FA obtained by EDS test

resistance 120.0±0.3 Ω, and gage factor 2.11±1% was applied. The data logger was programmed in LabVIEW with five strain channels. The experimental procedure of residual stress measurement was conducted at room temperature. The metal band saw cutter model BT-MB 550 U: Einhell Brand was used to cut the samples, while a strain gage senses the strain vs time simultaneously within the samples. Then the data logger recorded the results using DIAdem software. The cutting process was achieved at a depth of cut (12 mm) and a cutting time 11.3 s. Through the cutting operation, cooling liquid was utilized to prevent heat generation, which could affect the accuracy of strain measurement. The residual stresses were calculated based on the measured strain using Hook's law (4). The residual stresses were measured for samples before and after ECAP at two angles, 120° and 135°, for 1, 2, 4, and 6 passes. Figure 2 presents the CT for residual stress measurement.

The specimens used for microstructure evaluation were cleaned of grease, oil, and dust, then cut off 5 mm from the middle of the specimen, followed by grinding with silicon carbide paper from 180 to 2000 grit, then polished with a velvet cloth. For more accurate information about the surface morphology of hybrid aluminum composite before and after ECAP with high resolution of surface texture, shape, topography, and magnification, the SEM was applied The specimen was exposed to gold water coating using a single-target plasma device, which facilitates accurate inspection of the surfaces. The testing was conducted by the SEM device (INSPECT S50).

## RESULTS AND DISCUSSION

Figure 3 presents the residual stresses measurement in the axial direction obtained by the destructive procedure based on the CT along the depth of the cut when the ECAP angle was 120° at various cycles. It can be seen that the residual stresses were in compressive mode near the surface of the composite rod, while they were in tensile behavior around the rod center for all passes of ECAP, as well as the casting rod (initial rod). The low magnitudes of these stresses were recorded at the initial rod due to the effect of the heat through the casting operation that was applied to manufacture the composite rod. On the other hand, the increase in the value of residual stresses occurred at the first pass of ECAP due to the impact of the cold forming process that led to the creation of plastic deformation, and then the generation of residual stresses (3–5). The shear direction of the internal stresses that were produced due to the impact of the compression force to extrude the hybrid aluminum composite (Al1050/$B_4C$/FA) through the ECAP is considered an important factor in determining the behavior of the residual stresses. The compression forces were determined to be 61, 65, 68, 72, 76, and 88 kN for the passes 1P, 2P, 3P, 4P, 5P, and 6P, respectively. From Figure 3, the high values for the tensile state (positive sign) of the residual stresses were at four cycles of ECAP, while the high magnitudes of compressive residual stresses (negative sign) were measured at pass one of ECAP.

Figure 4 shows the relationship between residual stresses and depth of cut at different cycles of ECAP when the channel angle of forming was

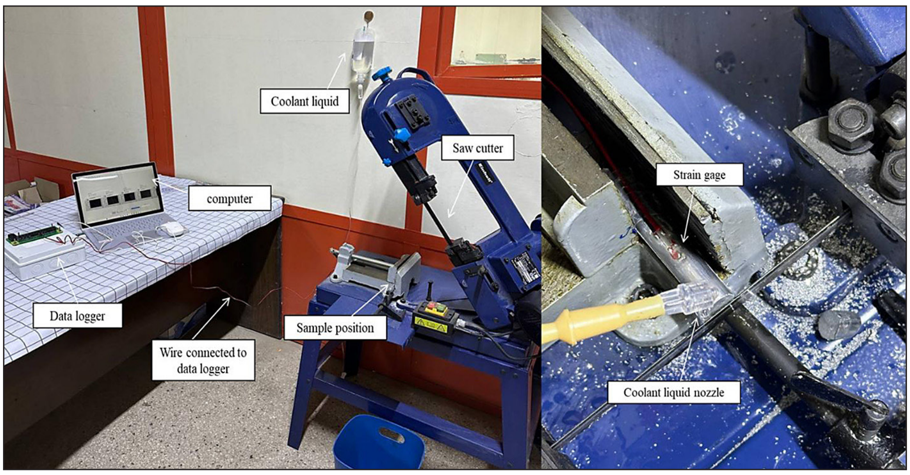


**Figure 2.** Cutting technique (CT) for residual stress measurement

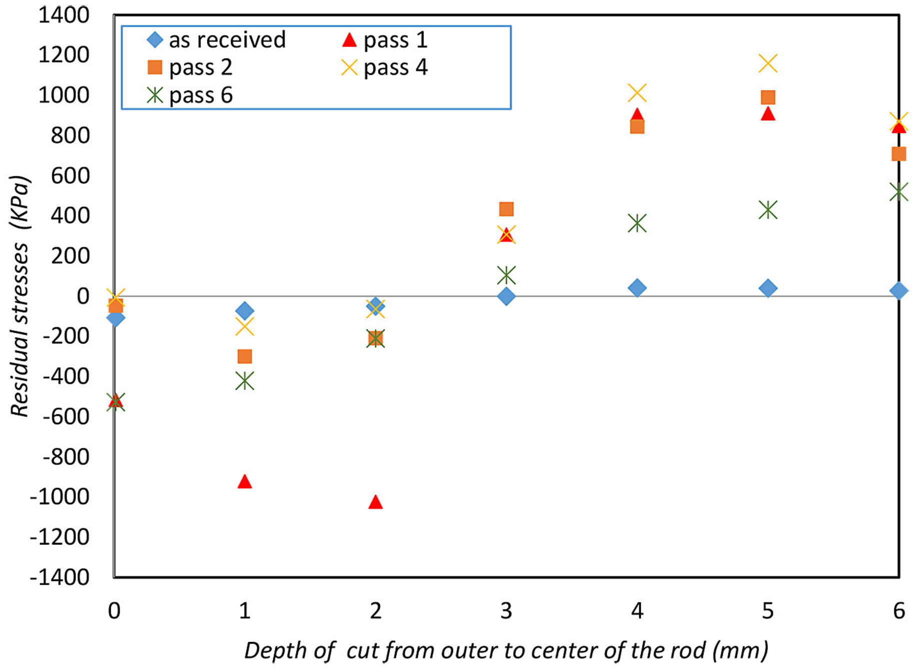


**Figure 3.** Results of residual stresses of Al1050/$B_4C$/FA composite obtained by CT at ECAP angle of 120°

135°. Both the numbers of passes 4 and 6 gave high values of tensile residual stresses near the surface of the rod because of the effect of shear stresses. In the country, high magnitudes of compressive stresses were recorded at the first pass of ECAP. Similar to Figure 3, the initial rod that was subjected to the thermal casting process has minimum values of residual stresses compared to all ECAP cycles. The compression force has a strong effect on the generated residual stresses due to the plastic deformations that take place through the forming process (3). The compression forces were measured at 58, 63, 66, 70, 74, and 79 kN at the number of passes 1P, 2P, 3P, 4P, 5P, and 6P in order.

Based on Figures 3 and 4, it can be observed that the effect of the number of ECAP cycles strongly affects the magnitudes of the residual stresses, which correlate with the impact of shear stresses due to the compression force impact. In the cold forming process, the state of the residual stresses depends on the amount of reduction area as presented in (25). In this work, there was no change in the area of the rod before and after ECAP; therefore, the state and behavior of residual stresses were almost the same for all cycles of ECAP. The impact of the difference in the angle of the channel ECAP (120° and 135°) is quite small compared to the number of passes.

Figure 5 visualizes the images of the rod composite obtained by SEM before and after ECAP passes (2, 4, and 6) with a channel angle of 120°. The casting material Al1050/$B_4C$/FA composite exhibited nonhomogeneous particle distribution with few cracks and pores, see Figure 5a. Coarse grains for the initial sample were observed, ranging between 4–15 μm. Figure 5b shows the microstructure of Al1050/ $B_4C$/FA composite after two cycles for channel angle 120°, where the grains are subject to significant elongation due to severe plastic deformation that forms a lamellar structure along the deformation direction. The grain size after 2 passes was reduced to 2–12 μm. The grains undergo subsequent refinement, represented in Figures 5c and 5d, reaching 2–10 μm after 4 passes at 120° and 1–8 μm after 6 passes, indicating the progressive influence of SPD on microstructure refinement.

Figure 6 illustrates the microstructural images of the hybrid aluminum composite as cast rod and after undergoing SPD at 135° die angle using SEM. The grain size reduction has varied with the number of ECAP cycles, which influenced the strain accumulation and materials flow as presented in Figure 6b. After two passes at 135°, the grain size of Al1050/$B_4C$/FA ranged from 4–15 μm, demonstrating lower refinement compared with the second pass by 120° of the die angle. Moreover, the grain refined further was recorded in the range of 3–11 μm as introduced in Figure 6c, while the grain size after six ECAP passes at 135°, measuring 2–9 μm as depicted in Figure 6d. Based on Figures 5 and 6, the grain size of the composite rods

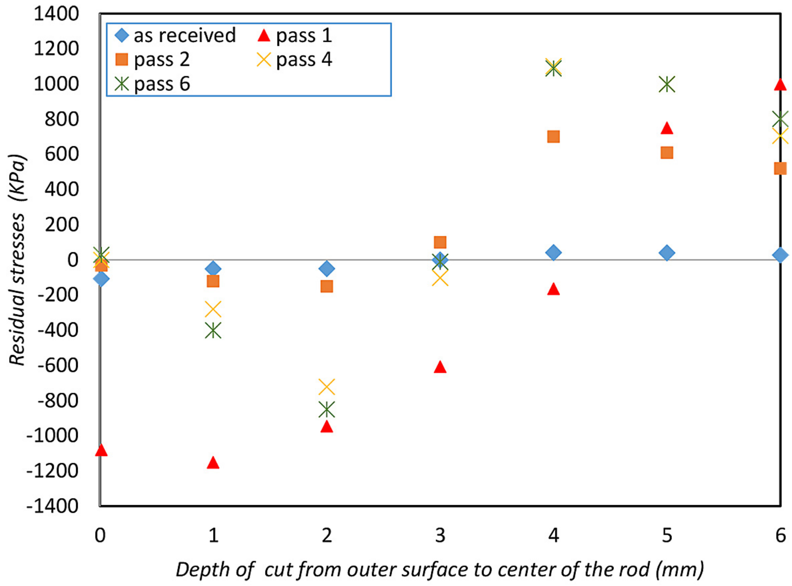


**Figure 4.** Results of residual stresses of Al1050/$B_4C$ /FA composite obtained by CT at ECAP angle of 135°

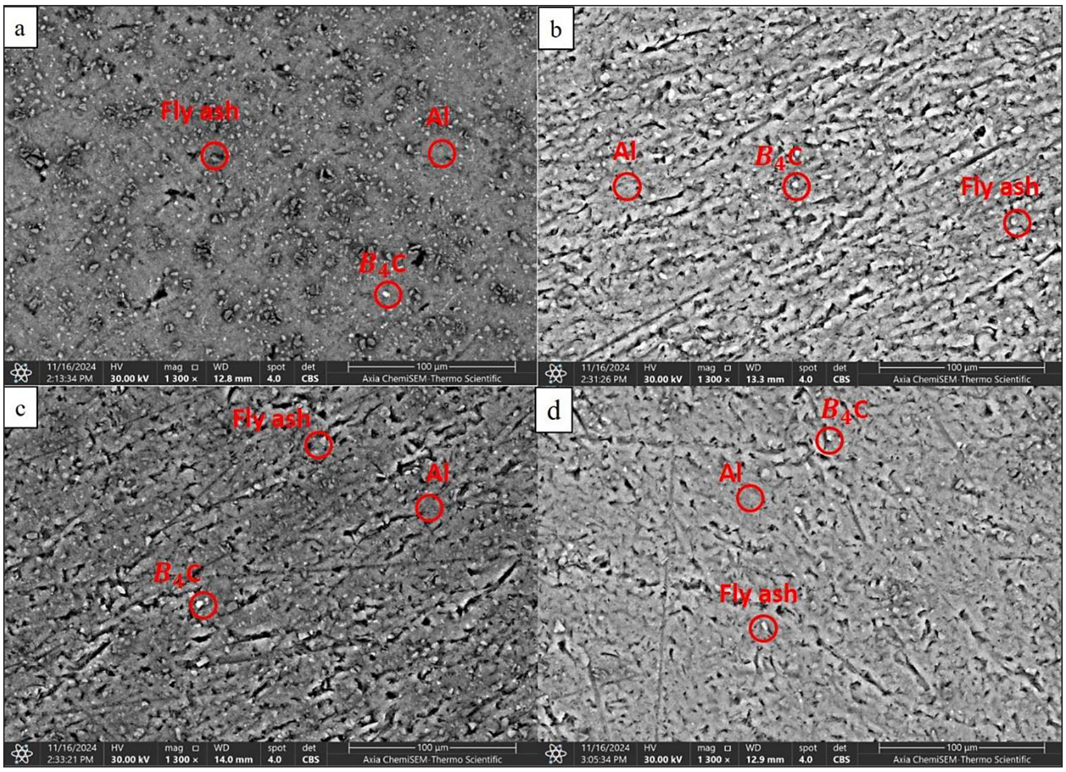


**Figure 5.** Results of the microstructure of Al1050/$B_4C$/FA obtained by SEM at the channel angle ECAP of 120° when (a) as cast, (b) 2 passes, (c) 4 passes, and (d) 6 passes

was determined by the ImageJ software. Although the reduction in grain size was greater at 120° die angle than 135° due to the amount of high deformation force induced at 120°, both ECAP die angles exhibit similar behavior, the reduction of grain size and enhancement of the defects increase with an increase in the number of ECAP cycles.

## CONCLUSIONS

In this work, the effect of SPD by different ECAP cycles at two channel die angles, 120° and 135°, on the residual stresses and microstructure of Al1050/$B_4C$ /FA hybrid aluminum composite produced by the stir casting route was established.

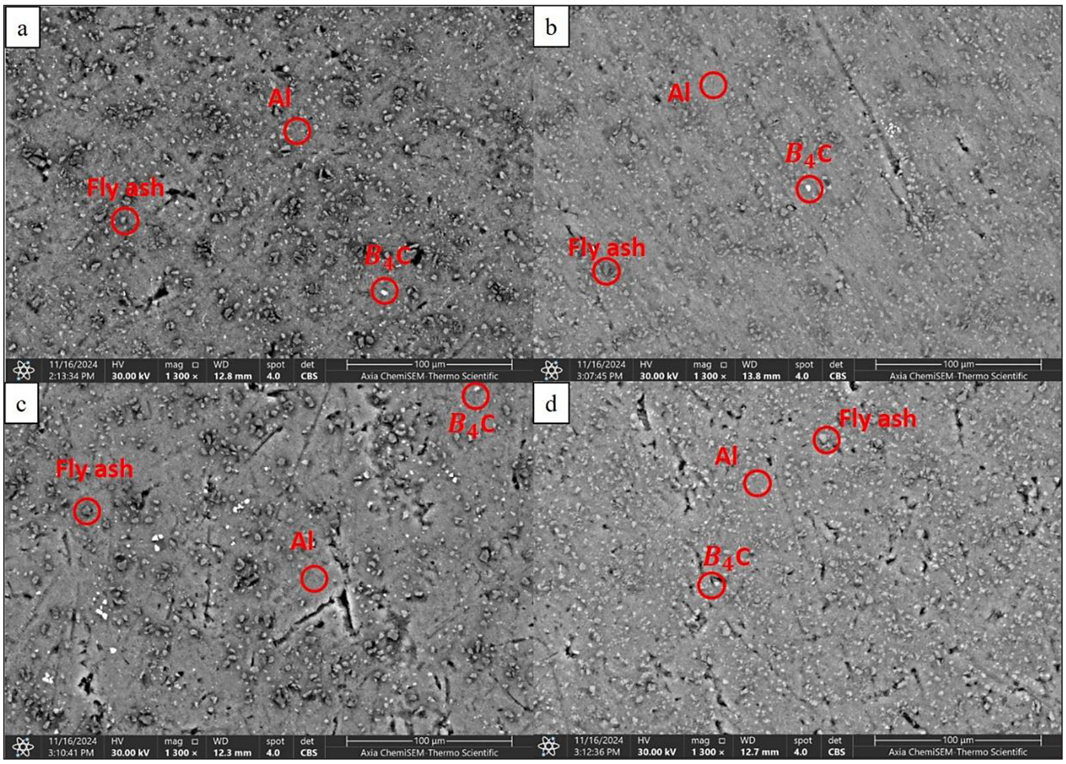


**Figure 6.** Results of the microstructure of Al1050/$B_4C$/FA obtained by SEM at the channel angle ECAP of 135° when (a) as cast, (b) 2 passes, (c) 4 passes, and (d) 6 passes

The findings obtained in this investigation were summarized as follows:
1. The residual stress values increase at the near and center of the rod when the rod is subjected to SPD, and they change at various cycles of ECAP.
2. The state of axial residual stresses is in compression near the rod surface and a tension state near the rod center for all passes of ECAP.
3. Increasing the number of cycles affects the magnitude of residual stresses for both channel die angles, 120° and 135°, with nearly similar state (tension and compression) of the stresses for all passes.
4. The refinement of grain size can be increased in Al1050/$B_4C$/FA composite by increasing the number of ECAP cycles. The sixth pass gave more grain size reduction.
5. The channel die angle of 120° with the sixth pass of ECAP has an impact on the grain size reduction of the Al1050/$B_4C$/FA composite compared to 135°.

### Acknowledgments

The author offers sincere thanks to the "University of Diyala, College of Engineering" for helping in the experimental work.

## REFERENCES

1. Kumar KR, Kiran K, Sreebalaji V. Micro structural characteristics and mechanical behaviour of aluminium matrix composites reinforced with titanium carbide. Journal of Alloys and Compounds. 2017;723:795–801. https://doi.org/10.1016/j.jallcom.2017.06.309
2. Dhanesh S, Kumar KS, Fayiz NM, Yohannan L, Sujith R. Recent developments in hybrid aluminium metal matrix composites: A review. Materials Today: Proceedings. 2021;45:1376–81. https://doi.org/10.1016/j.matpr.2020.06.325
3. Gattmah J, Ozturk F, Shihab SK, Orhan S. Influencing the residual stresses in tubes drawn with a floating plug by changing tool parameters. Journal of the Brazilian Society of Mechanical Sciences and Engineering. 2022;44(7):298. https://doi.org/10.1007/s40430-022-03609-5
4. Gattmah J, Hussein EA, Jaseem AN, Shihab SK. Die angle effect on the generated residual stresses in the inclined and final region during the aluminum extrusion. Journal of Mechanical Science and Technology. 2024;38(8):4277–86. https://doi.org/10.1007/s12206-024-0724-6
5. Hussein EA, Gattmah J, Jaseem AN. Optimization of rolling parameters for enhancing the surface integrity of aluminum alloy. Journal of Harbin Institute of Technology (New Series). 2023; https://doi.

org/10.11916/j.issn.1005-9113.2022115
6. Horn T, Silbermann C, Ihlemann J. FE-Simulation based analysis of residual stresses and strain localizations in ECAP processing. PAMM. 2017;17(1):309–10. https://doi.org/10.1002/pamm.201710124
7. Abd El Aal MI, Sadawy M. Influence of ECAP as grain refinement technique on microstructure evolution, mechanical properties and corrosion behavior of pure aluminum. Transactions of Nonferrous Metals Society of China. 2015;25(12):3865–76. https://doi.org/10.1016/S1003-6326(15)64034-1
8. Lokesh T, Mallik U. Effect of equal channel angular pressing on the microstructure and mechanical properties of hybrid metal matrix composites. Indian Journal of Science and Technology. 2016;9:1–7. https://doi.org/10.17485/ijst/2016/v9i35/88443
9. Lee HH, Gangwar KD, Park K-T, Woo W, Kim HS. Neutron diffraction and finite element analysis of the residual stress distribution of copper processed by equal-channel angular pressing. Materials Science and Engineering: A. 2017;682:691–7. https://doi.org/10.1016/j.msea.2016.11.094
10. Bharath A, Sundeep A, Sharan A, Reddy ASP, Phanibhushana M. Characterisation of aluminum metal matrix hybrid composites subjected to equal channel angular pressing. Materials Today: Proceedings. 2018;5(11):25396–403. https://doi.org/10.1016/j.matpr.2018.10.344
11. Romero-Resendiz L, Figueroa I, Reyes-Ruiz C, Cabrera J, Braham C, Gonzalez G. Residual stresses and microstructural evolution of ECAPed AA2017. Materials Characterization. 2019;152:44–57. https://doi.org/10.1016//j.matchar.2019.04.007
12. Sureshkumar P, Uvaraja V, Rajakarunakaran S. Addition of metallic reinforcement enhanced deformation and properties of ceramic reinforced composite by adapting ECAP with increment number of passes. Materials Research Express. 2019;6(8):086502. https://doi.org/10.1088/2053-1591/ab1b82
13. Hou X, Ban C, editors. Effect of ECAP on microstructure uniformity and mechanical properties of high purity aluminum. Journal of Physics: Conference Series; 2021: IOP Publishing. https://doi.org/10.1088/1742-6596/2021/1/012077
14. Güler Ö, Bağcı N, Güler SH, Canbay CA, Safa H, Yılmaz TA, et al. The effect of equal-channel angular pressing (ECAP) on the properties of graphene reinforced aluminium matrix composites. Journal of Composite Materials. 2021;55(13):1749–68. https://doi.org/10.1177/0021998320979040
15. Shivashankara B, Gopi K, Pradeep S, Rao RR, editors. Investigation of mechanical properties of ECAP processed AL7068 aluminium alloy. IOP Conference Series: Materials Science and Engineering; 2021: IOP Publishing. https://doi.org/10.1088/1757-899X/1189/1/012027
16. Al-Alimi S, Lajis MA, Shamsudin S, Yusuf NK, Chan BL, Didane DH, et al. Development of hot equal channel angular processing (ECAP) consolidation technique in the production of boron carbide (b4c)-reinforced aluminium chip (aa6061)-based composite. International Journal of Renewable Energy Development. 2021;10(3):607. https://doi.org/10.14710/ijred.2021.33942
17. Agarwal KM, Tyagi R, Choubey V, Saxena KK. Mechanical behaviour of Aluminium Alloy AA6063 processed through ECAP with optimum die design parameters. Advances in Materials and Processing technologies. 2022;8(2):1901–15. https://doi.org/10.1080/2374068X.2021.1878705
18. Sureshkumar P, Jagadeesha T, Natrayan L, Ravichandran M, Veeman D, Muthu S. Electrochemical corrosion and tribological behaviour of AA6063/$Si_3N_4$/$Cu(NO_3)_2$ composite processed using single-pass ECAPA route with 120 die angle. Journal of Materials Research and Technology. 2022;16:715–33. https://doi.org/10.1016/j.jmrt.2021.12.020
19. Sathi BR, Gurugubelli SN. The effect of ECAP on Structural Morphology and Wear Behaviour of 5083 Al Composite Reinforced with Red Mud. 2023. https://doi.org/10.5109/6792827
20. Tolcha MA, Gebrehiwot TM, Lemu HG. Enhancing mechanical properties of cast ingot Al6061 alloy using ECAP process. Journal of Materials Engineering and Performance. 2024:114. https://doi.org/10.1007/s11665-024-09978-3
21. Hassan AM, Gattmah J, Shihab SK. Evaluation of microstructure and mechanical properties of Al1050/$Al_2O_3$/Gr composite processed by forming operation ECAP. Open Engineering. 2024;14(1):20240041. https://doi.org/10.1515/eng-2024-0041
22. Canute X, Majumder M. Mechanical and tribological behaviour of stir cast aluminium/boron carbide/fly ash composites. Journal of Engineering Science and Technology. 2018;13(3):755–77.
23. Bhowmik A, Kumar R, Babbar A, Romanovski V, Roy S, Patnaik L, et al. Analysis of physical, mechanical and tribological behavior of Al7075-fly ash composite for lightweight applications. International Journal on Interactive Design and Manufacturing (IJIDeM). 2024;18(6):3699–712.
24. Sathish S, Nair A, Sundaraselvan S. Investigation on mechanical properties of aluminum hybrid matrix composites reinforced with fly ash and titanium diboride using stir casting technique. Materials Research Express. 2024;11(7):076523. https://doi.org/10.1088/2053-1591/ad6238
25. Gattmah J, Ozturk F, Orhan S. Experimental and finite element analysis of residual stresses in cold tube drawing process with a fixed mandrel for AISI 1010 steel tube. The International Journal of Advanced Manufacturing Technology. 2017;93:1229-41. https://doi.org/10.1007/s00170-017-0583-8